J. Math. Biol. 41, 430–454 (2000)
Digital Object Identifier (DOI):
10.1007/s002850000022

Mathematical Biology

M.A. Lewis

Spread rate for a nonlinear stochastic invasion

Received: 19 October 1998 / Revised version: 1 September 1999 /
Published online: 4 October 2000 –

Abstract. Despite the recognized importance of stochastic factors, models for ecological invasions are almost exclusively formulated using deterministic equations [29]. Stochastic factors relevant to invasions can be either extrinsic (quantities such as temperature or habitat quality which vary randomly in time and space and are external to the population itself) or intrinsic (arising from a finite population of individuals each reproducing, dying, and interacting with other individuals in a probabilistic manner). It has been long conjectured [27] that intrinsic stochastic factors associated with interacting individuals can slow the spread of a population or disease, even in a uniform environment. While this conjecture has been borne out by numerical simulations, we are not aware of a thorough analytical investigation.

In this paper we analyze the effect of intrinsic stochastic factors when individuals interact locally over small neighborhoods. We formulate a set of equations describing the dynamics of spatial moments of the population. Although the full equations cannot be expressed in closed form, a mixture of a moment closure and comparison methods can be used to derive upper and lower bounds for the expected density of individuals. Analysis of the upper solution gives a bound on the rate of spread of the stochastic invasion process which lies strictly below the rate of spread for the deterministic model. The slow spread is most evident when invaders occur in widely spaced high density foci. In this case spatial correlations between individuals mean that density dependent effects are significant even when expected population densities are low. Finally, we propose a heuristic formula for estimating the true rate of spread for the full nonlinear stochastic process based on a scaling argument for moments.

1. Introduction

Biological invasions are more complex than the deterministic mathematical models indicate. Not only are there spatial and temporal variations in factors affecting spread, but the observed density of organisms rarely can be described by a simple expanding wave front; rather, it is typical to observe a series of invaded patches which spread, coalesce and spawn new patches [30]. This can be seen clearly for

M.A. Lewis*: Department of Mathematics, University of Utah, JWB 233, Salt Lake City, UT 84112, USA. e-mail: mlewis@math.utah.edu

*Research supported in part by the National Science Foundation under grant no. DMS-9457816, by the Institute for Mathematics and its Applications with funds provided by the National Science Foundation, and by a fellowship from the Alfred P. Sloan Foundation.

Key words: Moment closure – Covariance – Integrodifference – Nonlinear stochastic process – Invasion – Spread rate

species as diverse as cheat grass (*Bromus tectorum*), and house finch (*Carpodacus mexicanus*) [15].

Stochastic factors play a key role here. In a spatially homogeneous environment, stochastic movements of individuals affect the location of the patches of individuals. This can be seen by modeling the behavior of individuals with a branching process where individuals have given probabilities of reproducing and dying per unit time and redistribute spatially. Using Monte Carlo simulations of the branching process we show in Figure 1a and 1b that long distance dispersal over multiple space scales

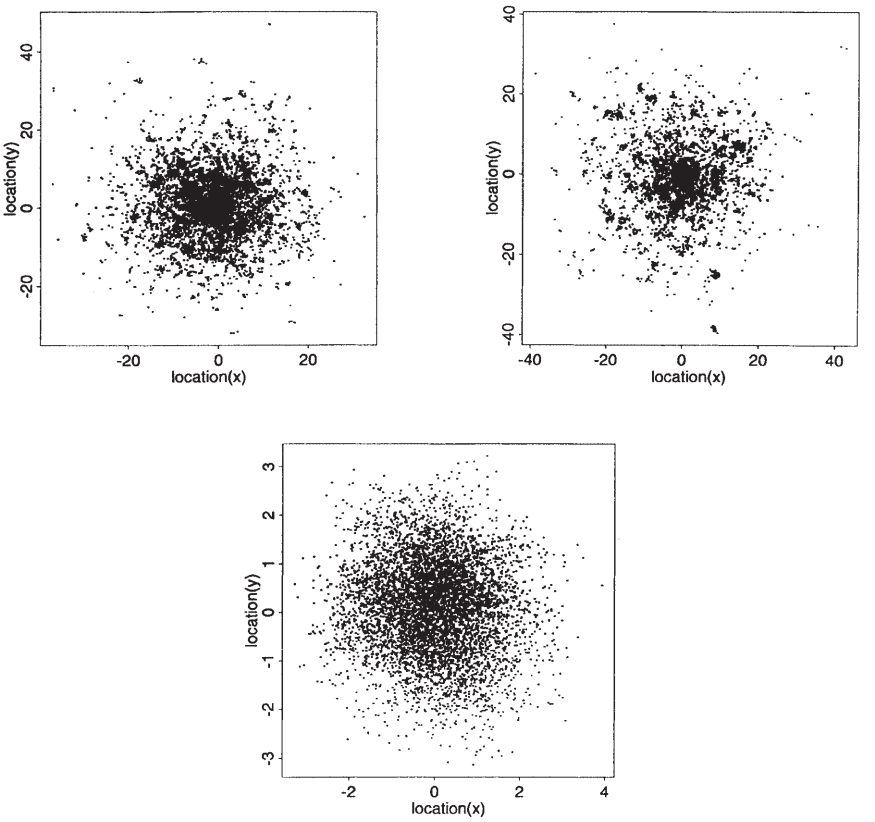

Fig. 1. Monte-Carlo simulation of reproducing dispersing individuals. Each time step: (i) individuals have a Poisson number of offspring, with mean of 1.5, (ii) offspring disperse with random distances drawn from a redistribution kernel $k(x)$. Angles are drawn from a uniform distribution, and (iii) the parent individual then dies. Initially 20 individuals were released at $x = 0$. The distribution of individuals is shown after 15 time steps for simulations. Figures (a) and (b) use a composite Normal redistribution kernel (9) with $\sigma_1 = 0.3606, \sigma_2 = 9.2878$ and $p = 0.9$. This gives an expected dispersal distance of one unit and a maximum value of $k(0) = 1$. The only difference between the simulations shown in (a) and (b) is the random number seed used. Figure (c) eliminates the long-distance dispersal component by using the same kernel, but with $p = 1.0$. Notice the different spatial scale for spread when the long-distance component is eliminated.

yields spatial correlations between individuals as evidenced by 'patchy' spread, with the locations of patches varying from simulation to simulation. Here individuals are not interacting with each other; each of them is simply reproducing and dispersing according to simple probabilistic rules given in the figure legend. The spatial correlations evident in this kind of spread are discussed in detail in a recent paper by Lewis and Pacala [20]. In this paper we concern ourselves with the role of such spatial correlations in slowing the one-dimensional spatial spread of a population subject to intrinsic stochastic factors and interacting spatially in a nonlinear fashion.

The measure of the rate of spread we will use here is the so-called 'expectation velocity' [27]. This can be described as the speed of movement c of a point x_t beyond which the expected number of individuals n_e is fixed. Thus x_t is defined so that the integral of the expected density over the interval (x_t, ∞) is n_e. Here expectation is taken over the entire ensemble of realizations of the stochastic process. For example, to compute x_t numerically over m Monte-Carlo simulations one simply tracks the location of the $m \times n_e$th individual from the right as a function of time over m combined Monte-Carlo simulations (see Figures 3 and 4 for actual calculations). While a typical invasion scenario would give rise to two such 'farthest dispersing individuals', one to the right and the other to the left, without loss of generality we simply consider the rightward moving wave.

Other definitions of spread rates are given by

1. The speed of movement of a point x_t at which the expected density of individuals n_e is fixed [27]. This alternate definition of the expectation velocity will coincide with our definition in the previous paragraph if the spreading population forms a traveling wave – a translation invariant profile shifting to the right at the given speed. Mollison [27] also argues that the two expectation velocity definitions should coincide for linear stochastic processes and some nonlinear stochastic processes.
2. The rate of change of the average location of the farthest forward individual with respect to time [6]. McKean [24] showed that, in certain linear stochastic processes, the distribution of the furthest forward individual can be modeled by a nonlinear deterministic reaction-diffusion equation (KPP or Fisher equation), which in turn exhibits traveling wave solutions.

It is known that simple nonlinear spatial lattice models support waves with a constant asymptotic spread rate [7] and these rates have been approximated analytically using pair-edge approximations [10]. Also, Mollison [28] showed almost sure convergence of the 'furthest-forward' velocity for a general dispersal function with exponentially bounded tail. This result relies upon population monotonicity – if an individual dies through nonlinear interactions it is only because there is another individual at the same lattice point already. However, our interest in this paper is in nonlinear stochastic processes in *continuous* space and discrete time (as described below). It has not been shown mathematically when or if such models have an asymptotically constant rate of spread. The result of Mollison cannot be applied directly here, not only because space is continuous, but also because the discrete time dynamics can actually violate the monotonicity

condition – two individuals that crowd each other will both die in a single time step. We conjecture that the spread in such models does asymptotically achieve a constant rate under certain conditions on the dispersal process (Conjecture 1 in Section 7) and provide numerical evidence for this conjecture (Section 7).

Our approach in this paper is to derive an approximate deterministic model which describes the first two spatial moments of the nonlinear stochastic process: expected density and expected joint density. This model is not closed – unknown higher order moments are needed to solve for the first two moments. By eliminating various terms in the equations, we close the system and provide two new 'models'. The solution to the first yields an upper bound for expected density and the solution to the second provides a lower bound. A constant asymptotic spread rate is calculated for the upper solution. The lower solution is shown to be valid for small time, but invalid for large time. However, a formal calculation of the asymptotic spread rate formula for this case indicates the qualitative role of competition with relatives in slowing the wave. We propose a heuristic modification of this spread rate formula based on a moment closure approximation. We then use this heuristic formula to estimate the asymptotic spread rate of the nonlinear stochastic process and then compare our estimates to numerical results from Monte-Carlo simulations.

2. A discrete-time deterministic model

Here individuals first undergo reproduction and then redistribute their offspring according to a dispersal function, before reproduction occurs once again. If generations are non-overlapping, as is the case with annual plants and many insect species, the process is described by

$$N_{t+1}(x) = \int_{-\infty}^{\infty} k(z-x)\, f(N_t(z))\, dz, \tag{1}$$

where $N_t(x)$ is the density of individuals at point x and time t. Density-dependent fecundity is described by the nonlinear map $f(N)$ with equilibria at extinction ($N = 0$) and carrying capacity ($N = N^*$) so that $f(0) = 0$ and $f(N^*) = N^*$. Dispersal is described a kernel or dispersal function, $k(z-x)$, which depends upon the distance $|z - x|$ between the location of birth z and the location of settlement x so that

$$k(z-x)\Delta z\Delta x = \text{Probability of dispersing from } \Delta z \text{ about } z \text{ to } \Delta x \text{ about } x. \tag{2}$$

Equation (1) states that the density of offspring at point z (denoted by $f(N_t(z))$, multiplied by the dispersal function (denoted by $k(z-x)$) and then integrated over all possible locations z in the study area, yields the density of individuals at the next time step $N_{t+1}(x)$. Historically integrodifference models have been used to predict changes in gene frequency [35,38,37,22,21,23] and only more recently have they been applied to ecological problems [17,12,13,16,18,11,14,32].

A detailed analysis of wave speeds for integrodifference models can be found in the papers of Weinberger [37,38]. To summarize some key results from Weinberger's analysis: providing $f(N) \leq f'(0)N$ and $f'(N) \geq 0$ for all $N > 0$, and

the moment generating function of the kernel

$$\hat{k}(s) = \int_{-\infty}^{\infty} \exp(su)\, k(u)\, du \tag{3}$$

exists on some interval $[0, s_m)$, then

1. traveling wave solutions to (1) exist and have minimum wave speed

$$c_* = \min_{s>0} \left\{ \frac{1}{s} \log(R_0 \hat{k}(s)) \right\} \tag{4}$$

   where $R_0 = f'(0)$ is the basic reproductive ratio for the population ($R_0 > 1$).
2. the asymptotic speed of propagation of compact initial data $N_0(x)$ is c_*.

A heuristic understanding of the first result can be gleaned from a linear analysis about the leading edge of the wave of spread. This yields

$$N_{t+1}(x) = R_0 \int_{-\infty}^{\infty} k(z - x)\, N_t(z)\, dz. \tag{5}$$

The ansatz for a traveling wave solution moving at speed c is that $N_{t+1}(x) = N_t(x - c)$. Substitution into (5), multiplication by $\exp(sx)$ and integration yields a solvability criterion for nontrivial solutions

$$\exp(sc) = R_0 \hat{k}(s). \tag{6}$$

The minimum value of c that will satisfy this equation is given by $c = c_*$ in (4). In practice, the value of c_* and the corresponding value s_* can be calculated by the double-root condition

$$c\, \exp(sc) = R_0 \hat{k}'(s). \tag{7}$$

in conjunction with the solvability criterion (6) [19] (Figure 2). The corresponding value s^* satisfying (6)–(7) can be interpreted as the exponential rate of decay of the leading edge of the wave. To see this we observe that we would have come to the same solvability criterion (6) under the assumption that $N_t(x) \propto \exp(-sx)$ after deriving equation (5). Wave speeds lower than c_* give rise to complex values for s_* and give an oscillatory, and thus negative, leading edge to the wave. These wave speeds are excluded from consideration because they would lead to negative densities. The second result from Weinberger (above) indicates that compact initial data cannot converge to a wave moving at speed other than c_*. Henceforth we refer to c_* as the wave speed for (1).

The above argument that the asymptotic rate of spread of a nonlinear model is governed by the minimum speed for which the leading edge of the wave is non-negative is referred to as the *linear conjecture* [29,36] and is expected to hold if (a) an individual's reproduction in an 'occupied' environment is always less than in a 'virgin' environment, in other words, no Allee-like effects and (b) the influence of an individual on the environment far from its (present) position is negligible, in other words, no long-distance density-dependence. The linear conjecture has been used widely to calculate spread rates for single-species deterministic differential

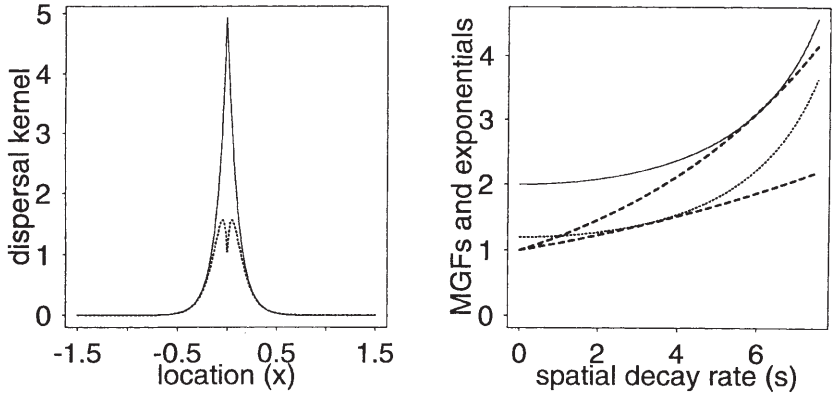

Fig. 2. Solvability criteria (6) and (25) calculated for a Laplace kernel $k(x) = \alpha \exp(-\alpha|x|)/2$. Figure (a) shows the dispersal kernel $k(x)$ (solid line) and dispersal kernel, corrected for interference from siblings $k(x) - \epsilon R_0 k^2(x)$ (dotted line). The corresponding moment generating functions (solid and dotted lines) and tangent exponential functions $\exp(c_*^+ s)$ for $c_*^+ = 0.105$ (lower dashed curve) and $\exp(c_* s)$ for $c_* = 0.19$ (upper dashed curve) are shown in Figure (b). Notice that $c_*^+ < c_*$.

and integral models and a similar approach has been applied to models for interacting species [31]. Note that the wave speed results of Weinberger (above) are independent of, but consistent with, the linear conjecture.

Typical kernels with moment generating functions include the Normal distribution and the exponential or Laplace kernel

$$k(x) = \frac{\alpha}{2} \exp(-\alpha|x|), \quad \alpha > 0. \tag{8}$$

When a proportion p of the individuals disperse locally and a proportion $1 - p$ disperse over a larger distance the relevant kernel may be given by a linear composition of Normal kernels:

$$k(x) = p\, N(0, \sigma_1^2) + (1 - p)\, N(0, \sigma_2^2). \tag{9}$$

This kernel can be derived by assuming that a proportion p of the individuals diffuse with a low diffusion coefficient D_1 for a unit time period and a proportion $1 - p$ of the individuals diffuse with a high diffusion coefficient D_2 over the same unit time period. The resulting distribution of individuals is given by (9) with $\sigma_1^2 = 2D_1$ and $\sigma_2^2 = 2D_2$. In the context of modeling invasions, Shigesada and coworkers referred to such diffusion over distinct spatial scales as 'stratified diffusion' [34].

The question arises as to the rate of spread of a solution to (1) when the redistribution kernel does not have exponentially bounded tails, in other words when the moment generating function (3) does not exist. Mollison [26] showed that, for this case, continuous-time contact distribution models can have asymptotically infinite rates of spread. This is also true for integro-difference models. The analysis for these models, including intermediate asymptotics on the rate of growth of the speed, is given by Kot and coworkers [19].

In this paper we use the traveling wave ansatz and a subsequent solvability criterion to evaluate wave speeds for linear 'multispecies' integrodifference models describing the nonlinear stochastic process. Here the 'species' are the spatial moments of the distribution of individuals. This analysis does not require recourse to a multispecies version of the linear conjecture (above) because the integrodifference models describing the nonlinear stochastic process are linear, although not closed. Thus, after deriving the models in Sections 3 and 4, we focus on how to 'close' the system (Sections 5 and 6) and, once this is done, the wave speed calculation is straightforward.

3. A discrete-time linear stochastic model

Stochastic models of population spread have been widely studied in the context of the spread of an infection. An introduction to the early work in this area can be found in a review by Mollison [27]. The idea that equations for 'second-order densities', such as spatial covariance, would yield information about the spread of an invading population was first pursued by Bartlett [2,3], and later by Daniels [8] and others [5]. Later approaches to nonlinear spatial epidemic models include particles interacting on a lattice [9] and coupling methods [1].

The simplest stochastic model involves only density-independent birth and dispersal. In this case equations for the successive moments can be written down explicitly (see [8] for a linear integro-differential equation formulation). Here we derive equations for the first two spatial moments for a population undergoing birth and dispersal in discrete time and continuous space.

We define $n(x)$ to be the expected density of individuals and $n^{(2)}(x, y)$ to be the expected joint density of individuals. Here expectation is taken over the ensemble of realizations for the stochastic process. Using these definitions, the spatial covariance density function is

$$c(x, y) = n^{(2)}(x, y) - n(x)n(y), \quad x \neq y \tag{10}$$

[4]. The correlation between locations of individuals is a scaled measure of this covariance.

If $\mathscr{R}$ is a random variable representing each individual's reproductive output, with expected value R_0 and variance σ^2, then equations governing the first two moments of a population undergoing distinct birth and dispersal events in discrete time are

$$n_{t+1}(x) = \int_{-\infty}^{\infty} R_0\, k(z - x)\, n_t(z)\, dz \tag{11}$$

and

$$\begin{aligned} c_{t+1}(x, y) = &\int_{-\infty}^{\infty} \left\{ R_0(R_0 - 1) + \sigma^2 \right\} n_t(z)\, k(z - x)\, k(z - y)\, dz \\ &+ \int_{\substack{-\infty \\ z_2 \neq z_1}}^{\infty} \int_{-\infty}^{\infty} R_0^2\, c_t(z_1, z_2)\, k(z_1 - x)\, k(z_2 - y)\, dz_1\, dz_2. \end{aligned} \tag{12}$$

where t is an index indicating the time step ($t = 0, 1, 2, \ldots$) [20]. After reproducing, the parents are assumed either to die, or to disperse, being indistinguishable from their offspring and included as part of their own reproductive output.

Equation (11) is simply a linear integrodifference equation for the expected density. It is identical to the linearized deterministic model (5), and thus the wave speed for (11) with compact initial data is given by (4). Hence the linear stochastic and the deterministic models have identical wave speeds, a well-known feature of spatial invasions [29].

The first term on the right hand side of (13) describes the spatial covariance due to two individuals having an identical parent, and the second term describes the spatial covariance due to two individuals from different but spatially correlated parents. Individuals are assumed to disperse independently from one another, and are only spatially correlated due to sharing a common ancestor. The expected number of ways to distribute indistinguishable siblings born at z to locations x and y is $E(\mathscr{R}(\mathscr{R}-1)) = R_0(R_0-1)+\sigma^2$. The birth rate variance σ^2 causes an increase in the contribution to spatial covariance that arises from individuals producing spatially correlated offspring. The case with a Poisson number of offspring yields $R_0(R_0-1)+\sigma^2 = R_0^2$. To keep the presentation clear in the remainder of the paper, we will assume that parents have a Poisson number of offspring unless stated otherwise.

4. A discrete-time nonlinear stochastic model

We now modify the linear stochastic model to include effects of local interactions. Specifically, we assume that, prior to reproduction, an individual at point x at time t inspects the neighborhood $(x-\epsilon/2, x+\epsilon/2)$ for other individuals. If there are others in this neighborhood the individual does not reproduce and dies. If there are no others in this neighborhood the individual has a Poisson number of offspring with mean R_0 and dies. These offspring then disperse according to the kernel k.

The expected number of other individuals in the neighborhood of size ϵ is

$$\int_{x-\epsilon/2}^{x+\epsilon/2} \frac{n_t^{(2)}(x,z)}{n_t(x)}\,dz \tag{13}$$

and the expected number of pairwise interactions between other individuals is

$$\int_{x-\epsilon/2}^{x+\epsilon/2}\int_{x-\epsilon/2}^{x+\epsilon/2} \frac{n_t^{(3)}(x,z_1,z_2)}{n_t(x)}\,dz_1\,dz_2. \tag{14}$$

Under the assumption that the joint and triple densities are order 1 we observe that equation (13) gives the approximate probability of having at least one other individual in the neighborhood, an approximation valid to $\mathcal{O}(\epsilon^2)$. The assumption that the spatial derivatives of $n_t^{(2)}$ are order 1 allows us to simplify (13) further, yielding the probability of having no other individuals in the neighborhood as

$$1-\epsilon\frac{\bar{n}_t^{(2)}(x)}{n_t(x)}+\mathcal{O}(\epsilon^2). \tag{15}$$

where

$$\bar{n}_t^{(2)}(x) = \lim_{z \to x} n_t^{(2)}(x, z) \tag{16}$$

is the expected *local* joint density.

Thus the nonlinear stochastic model is given to leading order of ϵ by

$$\begin{aligned} n_{t+1}(x) &= \int_{-\infty}^{\infty} R_0\, k(z-x)\, n_t(z) \left(1 - \epsilon \frac{\bar{n}_t^{(2)}(z)}{n_t(z)}\right) dz. \\ &= \int_{-\infty}^{\infty} R_0\, k(z-x)\, (n_t(z) - \epsilon \bar{n}_t^{(2)}(z))\, dz. \end{aligned} \tag{17}$$

The equation for the expected joint density now involves higher order moments, and is given to leading order of ϵ by

$$\begin{aligned} n_{t+1}^{(2)}(x, y) = & \int_{-\infty}^{\infty} R_0^2\, k(z-x)\, k(z-y)(n_t(z) - \epsilon \bar{n}_t^{(2)}(z))\, dz \\ & + \int_{\substack{-\infty \\ z_2 \neq z_1}}^{\infty} \int_{-\infty}^{\infty} R_0^2\, k(z_1 - x)\, k(z_2 - y)(n_t^{(2)}(z_1, z_2) \\ & - \epsilon \bar{n}_t^{(3)}(z_2, z_1) - \epsilon \bar{n}_t^{(3)}(z_1, z_2))\, dz_1\, dz_2. \end{aligned} \tag{18}$$

Here the local expected higher order density is given by

$$\bar{n}_t^{(3)}(z_1, z_2) = \lim_{z_3 \to z_1} n_t^{(3)}(z_1, z_2, z_3), \tag{19}$$

in a manner similar to (16). As with (13) the first term on the right hand side of (18) describes the joint density due to two individuals born of the same parent (siblings) and the second term describes the joint density due to two more distantly related individuals (cousins, second cousins and so forth). For the model to provide a valid description of the population each of these two terms must be non-negative. Notice that even though this system describes density-dependent interactions, it remains linear. However, it is not closed – the equation for $n_t^{(2)}(x, y)$ depends on higher order moments.

5. Moment closure and comparison methods

One approach to analyzing systems such as (17,18) is to 'close' the system, by making some assumptions about the higher order moments [33]. These higher order moments may be set to zero, or may be written as the product of lower order moments. The 'closed' system is then analyzed, and implications are made back to the 'open' stochastic system. One drawback to this approach is that moment closure methods are typically ad hoc, and it is thus difficult to draw a rigorous connection between the behavior of the 'open' and 'closed' systems.

Our approach in this section is to 'close' equation (18) by discarding certain terms. However, knowledge of the sign of the terms discarded will allow us to determine whether the expected density in the 'closed' system is an upper or lower

bound for the expected density in the 'open' system (17,18). Subsequent analyses of the spread rate for the upper solution will allow us to bound the spread rate for the full nonlinear stochastic system. Analysis of the lower solution will show that it is valid for small time values, but not for large time. None-the-less, we proceed to formally calculate a spread rate for the lower solution. This provides motivation for the heuristic analysis in Section 6.

5.1. An upper solution and its wave speed

One method of moment closure is to assume that density-dependent interactions only occur between siblings. Using $\bar{n}_t^{(2)}(x)$ to now denote the expected local joint density of siblings we simplify (18) to

$$\bar{n}_{t+1}^{(2)}(x) = \int_{-\infty}^{\infty} R_0^2\, k^2(z-x)(n_t(z) - \epsilon \bar{n}_t^{(2)}(z))\, dz. \tag{20}$$

Equations (17) and (20) thus yield an integrodifference model with two 'species': expected density and expected local joint density of siblings. Again, if the model is to provide a valid description of the densities, solutions to both of these equations must remain non-negative, a condition satisfied providing the local density experienced by individuals, $\bar{n}_t^{(2)}(z)/n_t(z)$, is $\mathcal{O}(1)$.

Intuitively we expect that ignoring density-dependent interactions with relatives more distant than siblings would lead to an overestimate of the expected density $n_t(x)$. This is indeed the case. More precisely, the solution $n_t^+(x) = n_t(x)$ to (17,20) provides a uniform upper bound for the solution $n_t(x)$ to (17,18). If the two systems of equations have identical initial data for the expected density and expected local joint density then $n_t^+(x) \geq n_t(x)$ for all x and t. This is a direct result of the corollary to the comparison theorem given in Appendix A in conjunction with the fact that the second term in (18) is nonnegative.

Equations (17,20) can be rewritten as

$$m_{t+1}(x) = \int_{-\infty}^{\infty} R_0(k(z-x) - \epsilon R_0\, k^2(z-x))m_t(z)\, dz, \tag{21}$$

where

$$m_t(x) = n_t(x) - \epsilon \bar{n}_t^{(2)}(x) \tag{22}$$

$$n_{t+1}(x) = \int_{-\infty}^{\infty} R_0 k(z-x) m_t(z)\, dz \tag{23}$$

Here we assume that $\epsilon R_0 k^{\max} < 1$, where $k^{\max}$ is the maximum value that the dispersal kernel $k(\cdot)$ attains. In other words, the neighborhood of interaction (ϵ) is small compared to the maximum density of offspring from a single parent ($R_0 k^{\max}$).

The linear system (21) has a form similar to (5) and thus analysis of this system yields a minimum wave speed of

$$c_*^+ = \min_{s>0} \left\{ \frac{1}{s} \log(R_0(\hat{k}(s) - \epsilon R_0 \hat{k^2}(s))) \right\}. \tag{24}$$

Here $\hat{k^2}(s)$ is the moment generating function of the squared dispersal kernel. Providing the dispersal kernel in (21) is nonnegative (as assumed above), this wave speed can be shown to be an upper bound on the rate of spread for compact initial data $m_0(x)$ (see [38], Theorem 6.3). Therefore, equation (23) indicates that the wave speed c_*^+ is also an upper bound on the rate of spread of expected density $n_t(x)$.

Alternatively, (24) arises from applying the heuristic approach in Section 2 directly to the linear system of two equations (17,20). The traveling wave ansatz is $n_{t+1}(x) = n_t(x-c)$, $\bar{n}_{t+1}^{(2)}(x) = \bar{n}_t^{(2)}(x-c)$. Substitution into (17,20), multiplication by $\exp(sx)$, integration and some algebra yields the solvability criterion

$$\exp(sc) = R_0(\hat{k}(s) - \epsilon R_0 \hat{k^2}(s)). \tag{25}$$

As in Section 2, the wave speed c_*^+ in (24) arises as a double root with respect to s of (25) (Figure 2).

In summary, we have results for (17,20) that are closely related to those given by Weinberger for single-variable nonlinear integro-difference equations (Section 2): traveling wave solutions have a minimum wave speed c_*^+ and the speed of propagation for compact initial data will not exceed c_*^+.

Note that as $\epsilon \to 0$ the minimum wave speed for the deterministic model (4) is recovered. The stochastic wave speed solvability criterion (25) can be thought of as a modification of the deterministic wave speed solvability criterion (6) where the moment generating function is taken not of the dispersal kernel $k(x)$, but of the kernel modified to reflect dispersal events that were unsuccessful due to the interference of siblings: $k(x) - \epsilon R_0 k^2(x)$. Because $k(x) - \epsilon R_0 k^2(x) \leq k(x)$ and is less that $k(x)$ over some nontrivial range of x, c_*^+ is strictly less than c_*.

A deterministic analog of (17) is

$$n_{t+1}(x) = \int_{-\infty}^{\infty} R_0\, k(z-x)\,(n_t(z) - \epsilon n_t^2(z))\, dz. \tag{26}$$

Here $\bar{n}_t^{(2)}$ is approximated by n_t^2. Such an approximation relies on the Law of Mass Action, which states that the probability of two individuals interacting is proportional to the product of their expected densities. This 'mean field' formulation is only valid if individuals have a random (Poisson) distribution in space. However the random distribution assumption is violated when correlations between individuals are present. For example, when spread is 'patchy' and there are positive correlations between individuals, $\bar{n}_t^{(2)} > n_t^2$, and thus the formulation (26) underestimates the strength of nonlinear interactions between individuals. In particular when the spread is 'patchy' we expect $n_t^{(2)}$ to be of the same magnitude as n_t in the leading edge of the wave, whereas $n_t^2 \ll n_t$ in the leading edge of the wave.

Although the nonlinear function in (26) does not satisfy Weinberger's [37,38] monotonicity constraint $f'(N) \geq 0$ for all $N > 0$, analysis about the leading edge of a wave solution to (26) still gives the deterministic minimum wave speed value c_* (4). This wave speed was confirmed numerically by simulating (26) for various dispersal kernels $k(x)$ by comparing the rate of movement of the leading edge of

the numerically simulated wave with c_* (4) calculated for the same $k(x)$. In fact, it is possible to use comparison methods in [37,38] to extend the wave speed result of Weinberger in Section 2 to single-humped (essentially quadratic) functions providing the map $N_{t+1} = f(N_t)$ remains positive for all initial data N_0 satisfying $f(N_0) > 0$ [19] (Lewis, Li and Weinberger, in preparation).

In conclusion, the wave speed c_*^+ for the upper bound lies below the wave speed c_* for the mean field approximation because the correlations between siblings slow the growth of the population, particularly at low densities, and thus the rate of spread of the population is decreased. Because solutions to the upper bound equations (17,18) spread no faster than c_*^+ this speed is an upper bound on the rate of spread of the nonlinear stochastic process.

5.2. A lower solution and its wave speed

A second method of moment closure is to assume that the expected third order density is zero in (18). This gives

$$n_{t+1}^{(2)}(x, y) = \int_{-\infty}^{\infty} R_0^2\, k(z-x)\, k(z-y)(n_t(z) - \epsilon \bar{n}_t^{(2)}(z))\, dz + \int_{\substack{-\infty \\ z_2 \neq z_1}}^{\infty} \int_{-\infty}^{\infty} R_0^2\, k(z_1 - x)\, k(z_2 - y)\, n_t^{(2)}(z_1, z_2)\, dz_1\, dz_2. \quad (27)$$

This assumption implies that lineages of relatives more distant than siblings have not been regulated by nonlinear interactions with other individuals since they interacted with siblings at birth or since $t = 0$, whichever is more recent. This assumption is potentially flawed as it leads to unbounded geometric growth of $n_t^{(2)}(x, y)$ in (27) and hence to violation of our modeling requirement in Section 4 that $n_{t+1}^{(2)}(x, y)$ be of order 1. The implications of this unbounded growth are discussed below. However, for now we assume that the model remains valid and proceed with the formal analysis.

Intuition would lead us to believe that ignoring nonlinear interactions in the lineages of distant relatives who may be now crowding a given individual will lead to underestimation of the expected density $n_t(x)$. As before, the intuitive expectation can be proved to be true. More precisely, the solution $n_t^-(x) = n_t(x)$ to (17,27) provides a uniform lower bound for the solution $n_t(x)$ to (17,18). If the two systems of equations have identical initial data for the expected density and expected local joint density then $n_t^-(x) \leq n_t(x)$ for all x. This is a direct result of the corollary to the comparison theorem given in Appendix A in conjunction with the fact that the expected third order density terms being non-negative means that the terms deleted from (18) are nonpositive.

Analysis of the wave speed for (17,27) is facilitated by using $\psi_t^{(i)}(x)$, the contribution to the expected local joint density $\bar{n}_t^{(2)}(x)$ from pairs of individuals with their most recent common ancestor at time i ($i < t$). The simplest case arises from a single individual released at the point $x = 0$ at time $t = 0$ so that $n_0(x) = \delta(x)$,

$\bar{n}_0^{(2)}(x) = 0$. In this case (27) can be rewritten as

$$\psi_{i+m}^{(i)}(x) = \int_{-\infty}^{\infty} R_0^{2m}\, k_{m-1}^2(z-x) \left(n_i(z) - \epsilon \sum_{j=0}^{i-1} \psi_i^{(j)}(z) \right) dz \qquad (28)$$

(Appendix B). Here we define the sum in (28) to equal zero when $i = 0$. Thus (17,27) can be rewritten as

$$n_{t+1}(x) = \int_{-\infty}^{\infty} R_0\, k(z-x) \left(n_t(z) - \epsilon \sum_{i=0}^{t-1} \psi_t^{(i)}(z) \right) dz. \qquad (29)$$

$$\psi_t^{(i)}(x) = \int_{-\infty}^{\infty} R_0^{2(t-i)}\, k_{t-i-1}^2(z-x) \left(n_t(z) - \epsilon \sum_{j=0}^{i-1} \psi_i^{(j)}(z) \right) dz, \quad (30)$$

where $k_0(x-y) = k(x-y)$ and k_j is the j-fold convolution of k with itself:

$$k_j(x-y) = \int_{-\infty}^{\infty} \cdots \int_{-\infty}^{\infty} k(x-z_1)k(z_1-z_2)\cdots k(z_{j-1}-z_j) \times k(z_j-y)\, dx_1\, dx_2 \cdots dx_{j-1}\, dx_j, \qquad (31)$$

and, as before, we define the sums in (29)–(30) to equal zero when the final index in the sum lies below the first index. Applying the approach in Section 2 to the linear system (29,30) yields the solvability criterion

$$\exp(sc) = R_0 \hat{k}(s) - \epsilon \sum_{j=0}^{\infty} R_0^{2j+2} \hat{k}_j^2(s) \exp(-scj). \qquad (32)$$

The minimum wave speed c_*^- for this system, providing it exists (see below), is calculated as the value $c = c_*^-$ for which (32) has second order root (with respect to s). The corresponding value of s, given by $s = s_*^-$, is the exponential decay of the leading edge of the wave. Notice that if we truncate the infinite series in (32) after the first term then we regain (25).

Again, the stochastic wave speed solvability criterion (32) can be thought of as a modification of the deterministic wave speed criterion (4) where the moment generating function is taken not of the dispersal kernel $k(x)$, but of the kernel modified to reflect dispersal events that were unsuccessful due to the interference of all possible relatives:

$$k(x) - \epsilon \sum_{j=0}^{\infty} R_0^{2j+1} k_j^2(x + jc). \qquad (33)$$

The first term of the sum in (33) describes interference to reproduction by siblings, the second term describes interference by cousins and so on. The argument $x + jc$ to the dispersal kernel in (33) accounts for the wave having moved distance c per time step. The interference effect of distant relatives is overestimated in this formula as it is assumed that they have not been regulated by nonlinear interactions with other

individuals since they interacted with their siblings at birth. The terms in the sum (32), evaluated at $s = 0$, may quickly grow to be larger that order 1. In fact the sum (32) is not guaranteed to converge – unbounded growth during the lineages of relatives more distant than siblings mean that the interference term itself can be unbounded.

6. Heuristic formula for the asymptotic rate of spread

As truncating the sum (33) after a single term leads to an underestimate of the total interference to reproduction by other individuals, and keeping all the terms in the sum leads to a severe overestimate of the interference, it is natural to ask whether truncating the sum after a few terms, or providing diminishing weight to successive terms in the sum, would provide a useful estimate for the asymptotic rate of spread of the stochastic process.

A typical moment closure approximation for (18) would be to replace the third order density by the product of the first and second so that

$$\begin{aligned} n_{t+1}^{(2)}(x, y) = & \int_{-\infty}^{\infty} R_0^2\, k(z-x)\, k(z-y)(n_t(z) - \epsilon \bar{n}_t^{(2)}(z))\, dz \\ & + \int_{\substack{-\infty \\ z_2 \neq z_1}}^{\infty} \int_{-\infty}^{\infty} R_0^2\, k(z_1 - x)\, k(z_2 - y) n_t^{(2)}(z_1, z_2) \\ & - (1 - \epsilon n_t(z_1) - \epsilon n_t(z_2))\; dz_1\, dz_2. \end{aligned} \tag{34}$$

However, employing the linear conjecture to calculate the wave speed leads to the linear equation (27). Thus the wave speed, providing it exists, is given by a double root with respect to s of the solvability criterion (32) and we would gain nothing by using this moment closure approximation. It can be reasoned that replacing $n_t^{(3)}$ in (18) with $n_t^{(2)} n_t$ in (34) implicitly assumes that $n_t^{(3)} \ll n_t^{(2)}$ and n_t in the leading edge of the wave, whereas in cases where the spread is 'patchy' we expect $n_t^{(3)}$ may be of the same magnitude as $n_t^{(2)}$ and n_t.

Another moment closure approximation for (18), that would permit $n_t^{(3)}$ to be of the same magnitude as $n_t^{(2)}$ and n_t at the leading edge of the wave, replaces the third order density by the quotient of squared second order density to the first order density so that

$$\begin{aligned} n_{t+1}^{(2)}(x, y) = & \int_{-\infty}^{\infty} R_0^2\, k(z-x)\, k(z-y)(n_t(z) - \epsilon \bar{n}_t^{(2)}(z))\, dz \\ & + \int_{\substack{-\infty \\ z_2 \neq z_1}}^{\infty} \int_{-\infty}^{\infty} R_0^2\, k(z_1 - x)\, k(z_2 - y) n_t^{(2)}(z_1, z_2) \\ & \times \left(1 - \epsilon \frac{n_t^{(2)}(z_1, z_2)}{n_t(z_2)} - \epsilon \frac{n_t^{(2)}(z_1, z_2)}{n_t(z_1)}\right) dz_1\, dz_2. \end{aligned} \tag{35}$$

Hence it would be implicitly assumed that the ratio of second to first order density gives the ratio of third to second order density. However, employing the linear conjecture to calculate the wave speed leads to an equation whose coefficients depend upon the ratio of $n_t^{(2)}$ to n_t at the leading edge of the wave, a ratio that we do not know.

An alternative approach is to make a heuristic estimate of this ratio at the leading edge of the wave and use it to estimate the value of

$$1 - \epsilon \frac{n_t^{(2)}(z_1, z_2)}{n_t(z_2)} - \epsilon \frac{n_t^{(2)}(z_1, z_2)}{n_t(z_1)} \tag{36}$$

at the leading edge of the wave for use in (35). The ratio $n_t^{(2)}(z_1, z_2)/n_t(z_1)$ can be interpreted as the expected density of individuals at point z_2, given that there is already an individual at the point z_1.

We consider the case where dispersal occurs over separate short and long length scales, such as shown in Figures 1a and 1b for the composite Normal kernel (9). Typically a lone colonizer will land in virgin territory at the leading edge of the wave, reproduce, and generate a small 'island' of closely related individuals (Figures 1a and 1b). This island will grow in size. As the growth occurs individuals will, on average, become more distantly related. Eventually, a long-distance colonizer will leave this 'island' and start a new 'island', thus repeating the process and moving the leading edge forward. The notion that the leading edge of the wave is comprised of 'islands' of individuals is particularly clear when the dispersal occurs over multiple length scales (compare Figure 1a and 1b with Figure 1c).

The expected density of individuals at point z_2, given that there is already an individual at the point z_1 therefore depends on the age of the island that the individual is in. For example, if the lone colonizer that started the island were the individual's parent, then the individual would only be surrounded by siblings. If the parent were at point z, then the expected density of siblings at point z_2 would be $R_0 k(z - z_2) \leq R_0 k_0^{\max}$, where $k_0^{\max}$ is the maximum value that $k_0(x)$ attains (see also equation (31)). As siblings disperse independently we simply bound $n_t^{(2)}(z_1, z_2)/n_t(z_1)$ above by $R_0 k_0^{\max}$, and (36) below by

$$\beta_1 = \max((1 - 2\epsilon R_0 k_0^{\max}), 0). \tag{37}$$

If the lone colonizer that started the island were the individual's grandparent, then the individual would only be surrounded by siblings and cousins. Thus $n_t^{(2)}(z_1, z_2)/n_t(z_1)$ would be bounded above by $R_0 k_0^{\max} + R_0^2 k_1^{\max}$, and (36) would be bounded below by

$$\beta_2 = \max((1 - 2\epsilon(R_0 k_0^{\max} + R_0^2 k_1^{\max})), 0). \tag{38}$$

Likewise, if the lone colonizer that started the island were the individual's great-grandparent, then the individual would only be surrounded by siblings, cousins and second cousins. Thus $n_t^{(2)}(z_1, z_2)/n_t(z_1)$ would be bounded above by $R_0 k_0^{\max} + R_0^2 k_1^{\max} + R_0^3 k_2^{\max}$, and (36) would be bounded below by

$$\beta_3 = \max((1 - 2\epsilon(R_0 k_0^{\max} + R_0^2 k_1^{\max} + R_0^3 k_2^{\max})), 0). \tag{39}$$

Continuing in this manner, if the lone colonizer that started the island were born m generations before the individual then (36) would be bounded below by β_m where $\beta_0 = 1$ and

$$\beta_m = \max\left(1 - 2\epsilon \sum_{j=1}^{m} R_0^j k_{j-1}^{\max}, 0\right). \tag{40}$$

for $m > 0$. Thus the appropriate value for (36) in equation (35) depends crucially upon the distribution of ages of 'islands' at the leading edge of the wave, a distribution we do not know *a priori*.

Our heuristic approach entails tracking interactions between individuals according to the time at which they shared their most recent common ancestor, as we did for equations (29) and (30) in Section 5.2. For the purpose of calculating interference to reproductive success from relatives we assume

Assumption 1. *The most recent common ancestor can be used to approximate the colonizer that started the 'island' on which both individuals are found.*

Assumption 2. *The factor β_m defined in (40) can be used to approximate the factor (36) in equation (35).*

Thus we use different values of β_m (40) for (36) in equation (35), depending upon the number of time steps previous at which the individuals shared their most recent common ancestor. Given that the most recent common ancestor was at time i, we assume that the island started at time step $t = i$. Thus at time step $t = i + 1$ all individuals on the island are siblings, so β_1 is an estimate for (36) in equation (35). At time step $t = i + 2$ we use β_2 as the estimate, and so on. This yields a modified version of (30)

$$\psi_t^{(i)}(x) = \int_{-\infty}^{\infty} \left(\prod_{m=0}^{t-i-1} R_0^2 \beta_m\right) k_{t-i-1}^2(z - x) \left(n_t(z) - \epsilon \sum_{j=0}^{i-1} \psi_i^{(j)}(z)\right) dz \tag{41}$$

(Appendix B). We assume that the leading edge of the wave asymptotically achieves a translation invariant 'traveling-wave' profile (see Conjecture 1 and related discussion in Section 7). Applying the approach in Section 2 to the linear system (29,41) yields the solvability criterion

$$\exp(sc) = R_0 \hat{k}(s) - \epsilon \sum_{j=0}^{\infty} R_0^{2j+2} \left(\prod_{m=0}^{j} \beta_m\right) \hat{k_j^2}(s) \exp(-scj). \tag{42}$$

Note that if all the β_m's were chosen to equal one this formula would simplify to equation (32). The minimum wave speed $\tilde{c}_*$ for equation (42) is calculated as the value $c = \tilde{c}_*$ for which (42) has second order root (with respect to s). The corresponding value of s, given by $s = \tilde{s}_*$, is the exponential decay of the leading edge of the wave. For this double root to yield the minimum wave speed in practice, we must check that the right hand side of the equation, evaluated at $s = 0$, exceeds 1. If it does not, a suggested modification to the heuristic formula (42) is to truncate

the terms from the sum for the highest values of m for which $\beta_m \neq 0$ until this condition is satisfied.

As before, the stochastic wave speed estimate $\tilde{c}_*$ can be thought of as a modification of the deterministic wave speed formula (4) where the moment generating function is taken not of the dispersal kernel $k(x)$, but of the kernel modified to reflect dispersal events that were unsuccessful due to the interference of all possible relatives:

$$k(x) - \epsilon \sum_{j=0}^{\infty} R_0^{2j+1} \left(\prod_{m=0}^{j} \beta_m \right) \hat{k}_j^2(x + jc). \tag{43}$$

Note that Assumption 1 yields an inexact approximation. For example, on an island three generations old, siblings and cousins do not provide the same interference to reproduction as on an island two generations old. However, Assumption 1 requires that, on each island, we calculate interference from siblings by assuming that the islands are 1 generation old, and, on each island, we calculate interference from cousins by assuming that the islands are 2 generations old. Similar assumptions are used when calculating interference to reproduction on islands more than three generations old. Assumption 2 also provides an inexact approximation. The parameter β_m is a lower bound for (36) and thus overestimates the nonlinear interactions with relatives, particularly when m is large and therefore $\beta_m = 0$. However, the formula (42) is the most accurate at the place where it is most crucial: at the leading edge of the wave, where the size of the islands is relatively small.

7. Comparison with Monte-Carlo simulations

We used extensive numerical simulations in evaluating (i) our conjecture that the leading edge of the wave achieves a constant expectation velocity asymptotically in time (Conjecture 1, stated below) and (ii) our analytical predictions for spread rates. Monte-Carlo simulations were run using NAG random number library routines in FORTRAN programs and are available to the reader upon request. Here we used the same composite Normal dispersal kernel and growth rate as in Figure 1a, except for a one-dimensional spatial process. The values of σ_1^2, σ_2^2 and p for this composite Normal kernel were chosen so as to give $k(0) = 1$ and an expected dispersal distance of 1. However, unlike Figure 1a, nonlinear stochastic interactions between individuals were also included. Initial conditions were given by 20 individuals released randomly in space within distance 5 of the origin at time $t = 0$. Each individual and its offspring were tracked explicitly in space and time.

Numerical evidence for a constant asymptotic expectation velocity for the leading edge of the nonlinear stochastic process is given in Figure 3. Here $\epsilon = 0.08$ and the average values of x_t are given for $n_e = 0.5$, 1.0, and 2.0. The average is taken over 10,000 Monte-Carlo simulations. Each line depicting x_t versus t achieves a similar slope by the time interval $40 \leq t \leq 50$, approximately 2.17 for $n_e = 0.5$, 2.18 for $n_e = 1.0$ and 2.18 for $n_e = 2.0$. As stated in the Introduction, we know of no *proof* that nonlinear stochastic processes considered here achieve a constant expectation velocity. However, based on these, and other, extensive numerical simulations we make the following conjecture

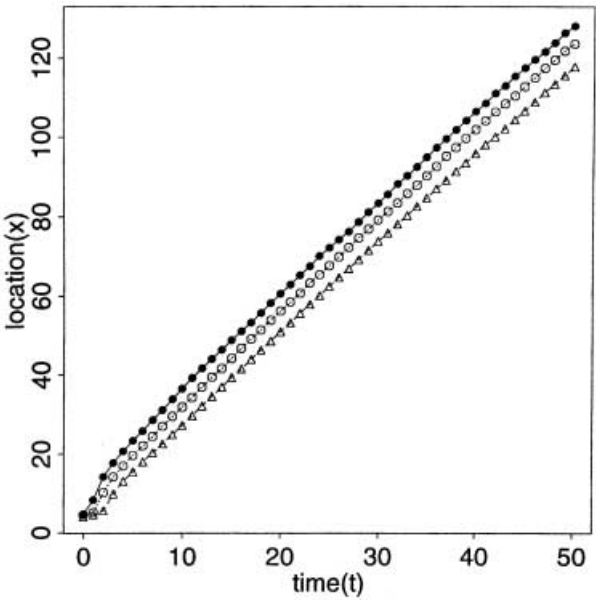

Fig. 3. Numerical evidence for a constant asymptotic expectation velocity for the nonlinear stochastic process. Here we used the same composite Normal dispersal kernel and growth rate as in Figure 1a, except now for a one-dimensional spatial process. Nonlinear spatial interactions were included, as described in Section 4, for $\epsilon = 0.08$. Average values of x_t are given for $n_e = 0.5$ (solid dots), 1.0 (open dots), and 2.0 (open triangles). The average is taken over 10,000 Monte-Carlo simulations. Each line depicting x_t versus t achieves a similar slope by the time interval $40 \leq t \leq 50$.

Conjecture 1. *For an exponentially bounded dispersal kernel $k(x)$ the leading edge of the nonlinear stochastic process described in Section 4 achieves a constant expectation velocity asymptotically in time. Using the terminology of Section 1, for n_e sufficiently small, $x_t \to$* constant *as $t \to \infty$.*

Because the speed is independent of the exact small value of n_e, the conjecture implies that the expectation achieves a translation invariant 'traveling wave form', at least locally at the leading edge of the wave. This property is used in Section 6.

We numerically calculated spread rates for $\epsilon = 0$, 0.02, 0.04, 0.06 and 0.08. Based on the results of the simulations shown in Figure 3 we used $n_e = 0.5$ and $40 \leq t \leq 50$ when evaluating asymptotic spread rates for the various values of ϵ. This interval was chosen as having a sufficiently large value of t to accurately estimate the speed, but a sufficiently small value of t to make the calculation feasible.

Table 1 and Figure 4 show numerical and predicted values for spread rates as ϵ varies. The case $\epsilon = 0$ has predicted spread rate $c_* = 3.69$. Appendix C gives details on calculating the moment generating function for the squared nth-fold convolutions of the composite Normal kernel and Table 1 gives the β_m values (40). These were needed to calculate $\tilde{c}_*$ in (42).

Table 1. Wave speed results for various neighborhood sizes ϵ. The values β_m, calculated from (40), are used in the formula for the estimated wave speed $\tilde{c}_*$ (32). The values of β_m were set to zero for $i \geq 7$ and $\epsilon = 0.02$ so as to satisfy the constraint that the right hand side of (42) evaluated at $s = 0$ exceeds 1. See the discussion in Section 6 for further details on this. The upper bound on the wave speed c_*^+ is calculated from (32) and the empirical wave speed $\hat{c}$ is calculated from Monte-Carlo simulations as described in Section 7 and Figure 4.

	β_1	β_2	β_3	β_4	β_5	β_6	β_7	c_*^+	$\tilde{c}_*$	$\hat{c}$	$\hat{c}/\tilde{c}_*$
$\epsilon = 0.02$	0.94	0.88	0.82	0.74	0.65	0.53	0	3.59	3.28	2.83	0.863
$\epsilon = 0.04$	0.88	0.76	0.64	0.48	0.29	0.06	0	3.49	2.99	2.65	0.886
$\epsilon = 0.06$	0.82	0.65	0.45	0.22	0	0	0	3.38	2.77	2.39	0.863
$\epsilon = 0.08$	0.76	0.53	0.27	0	0	0	0	3.27	2.57	2.17	0.844

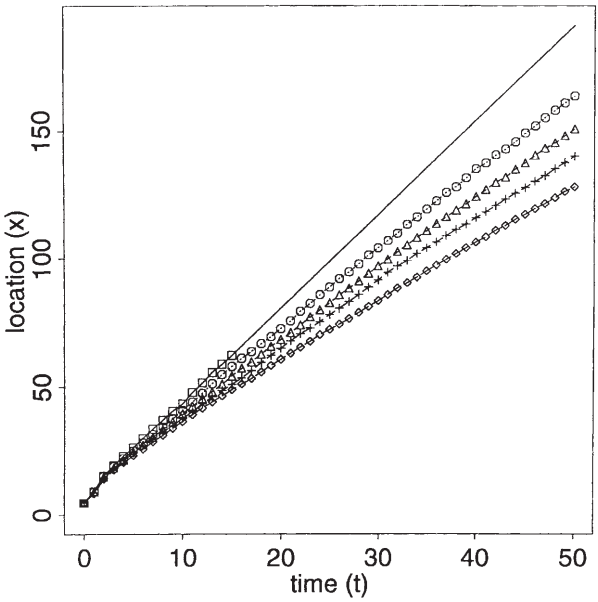

Fig. 4. Spread rates for various interaction neighborhoods ϵ. Average spread rates are shown for $\epsilon = 0.0$ (top), 0.02, 0.04, 0.06 and 0.08 (bottom). Calculations are made as in Figure 3. The number of Monte-Carlo simulations was $m = 2,000$ 2, 000, 4, 000, 6, 000 and 10, 000 for the values of ϵ, respectively. The additional simulations were made for larger ϵ because, at any given t, there were fewer individuals for these values of ϵ. The simulations for $\epsilon = 0$ were only given up to $t = 15$. The slope of the $\epsilon = 0$ line over the interval $10 \leq t \leq 15$ is 3.73. The curve is extended by a line of slope $c_* = 3.69$ for $15 \leq t \leq 50$. This truncation at time $t = 15$ was needed because the expected number of individuals at time $t = 50$ is 1.3×10^{10}.

Notice that the nonlinearities slow the wave dramatically: the case $\epsilon = 0.08$ has an asymptotic speed which is less than two thirds that of the case $\epsilon = 0$. The heuristic wave speed estimate $\tilde{c}_*$ is much closer to the numerical wave speed $\hat{c}$ than is the deterministic wave speed $c_* = 3.69$ or the upper bound on the wave speed c_*^+. For the ϵ values given here $\tilde{c}_*$ has a relative error $|(\tilde{c}_* - \hat{c})|/\hat{c}$ ranging from 11 to 16 %.

8. Discussion

This paper investigates the effect of nonlinear interactions on the spread rate of a stochastic process, a subject for which few rigorous analytical results exist. Our approach is to use various approximation methods to estimate the spread rate. We start with approximate equations describing spatial moments of the population, equations that are valid when the interaction neighborhood ϵ is small and the moments are order 1. Subsequent analysis of these equations yields upper and lower bounds on the expected density of individuals and an upper bound on the spread rate for the nonlinear stochastic process. The upper bound on the spread rate lies strictly below the spread rate for the equivalent nonlinear deterministic model. This bound makes more precise the belief that stochastic aspects of nonlinear interactions should slow spread rates (see [29]).

It is not known analytically under which conditions the nonlinear stochastic processes have constant spread rates. We conjecture that the leading edge of the wave achieves an asymptotically constant expectation velocity. This Conjecture 1, based on numerical simulations, implies that the leading edge of the wave achieves a translation-invariant 'traveling wave' profile. This translation invariance property is used in calculating a heuristic wave speed formula for the asymptotic expectation velocity, a formula that matches well with the numerical Monte-Carlo simulation results.

The key feature slowing spread of the nonlinear stochastic process is the covariance that arises between related individuals. The extreme case is evident in a population distributed in a collection of widely-spaced randomly located 'islands'. Here the expected density is low, but the likelihood of having a nearby neighbor is high. In terms of the variables of Section 4 $\bar{n}_t^2 \gg n_t^2$ and thus $c_t \gg 0$. Such 'island' patterns are especially likely in focal plant epidemics [30] such as potato blight [25], where very local patches of infestation or hot spots are separated spatially from other hot spots and are only connected through rare dispersal events in which a spore escapes the canopy. Thus the inclusion of higher order moments allows us to better describe the world 'as the individual perceives it' (in terms of the likelihood of having nearby neighbors), as opposed to the world as perceived through traditional deterministic models (in terms of expected density).

Acknowledgements. Thanks to Fred Adler, Jim Clark, Davar Khoshnevisan, Hans Metz and Rich McLaughlin for helpful comments and feedback. Thanks to David Eyre for his encouragement to get the paper written. Two anonymous referees provided helpful comments.

A. Comparison theorem

We compare solutions to

$$m_{t+1}(x) = \int_{-\infty}^{\infty} R_0\, k(z-x)\, \left(m_t(z) - \epsilon \bar{m}_t^{(2)}(z)\right)\, dz, \tag{44}$$

$$\bar{m}_{t+1}^{(2)}(x) = \int_{-\infty}^{\infty} R_0^2\, k^2(z-x)\, \left(m_t(z) - \epsilon \bar{m}_t^{(2)}(z)\right)\, dz + M_{t+1}(x) \tag{45}$$

with solutions to

$$n_{t+1}(x) = \int_{-\infty}^{\infty} R_0\, k(z-x)\, \left(n_t(z) - \epsilon \bar{n}_t^{(2)}(z)\right)\, dz, \tag{46}$$

$$\bar{n}_{t+1}^{(2)}(x) = \int_{-\infty}^{\infty} R_0^2\, k^2(z-x)\, \left(n_t(z) - \epsilon \bar{n}_t^{(2)}(z)\right)\, dz + N_{t+1}(x) \tag{47}$$

where both systems have identical initial conditions so that $n_0(x) = m_0(x)$ and $n_0^{(2)}(x) = m_0^{(2)}(x)$. These systems of equations only differ by the terms $M_{t+1}(x)$ and $N_{t+1}(x)$ in (45) and (47) respectively.

Theorem 1 (Comparison). *For* $t \geq 3$

$$m_t(x) = n_t(x) + \epsilon p_t(x) + \epsilon^2 R_0^2 \int_{-\infty}^{\infty} k^2(x-z)\, p_{t-1}(z)\, dz \tag{48}$$

where

$$\begin{aligned} p_t(x_0) \;&= N_t(x_0) - M_t(x_0) + \sum_{i=1}^{t-1} R_0^i \int_{-\infty}^{\infty} \cdots \int_{-\infty}^{\infty} (N_{t-i}(x_i) - M_{t-i}(x_i)) \\ &\quad \times \prod_{j=1}^{i} \left(k(x_{j-1} - x_j) - \epsilon R_0 k^2(x_{j-1} - x_j)\right)\, dx_2 \cdots dx_i. \end{aligned} \tag{49}$$

Proof. We define

$$\epsilon p_t(x) = (m_t(x) - \epsilon \bar{m}_t^{(2)}(z)) - (n_t(x) - \epsilon \bar{n}_t^{(2)}(x)), \tag{50}$$

verify equation (49) for the case $t = 2$ and then use induction on t to verify equation (49) for higher values of t. Lastly, equation (48) is given directly by the definition of p_t. □

Corollary 1. *If* $\epsilon R_0 k^{\max} < 1$, *where* $k^{\max}$ *is the maximum value that the dispersal kernel* $k(\cdot)$ *attains then, for any given time* t *and location* x,

1. *If* $N_s(y) \geq M_s(y)$ *for all times* $s \leq t$ *and all possible spatial locations* y *then* $m_t(x) \geq n_t(x)$, *and*
2. *if* $N_s(y) \leq M_s(y)$ *for all times* $s \leq t$ *and all possible spatial locations* y *then* $m_t(x) \leq n_t(x)$.

The condition $\epsilon R_0 k^{\max} < 1$ guarantees that the modified dispersal kernel $k(\cdot) - \epsilon R_0 k^2(\cdot)$ is nonnegative in equation (49). Hence the above inequalities follow directly from Theorem 1. We interpret the condition as meaning that the neighborhood of interaction (ϵ) is small compared to the maximum density of offspring from a single parent ($R_0 k^{\max}$). In other words, interactions between siblings are sufficiently weak.

B. Derivation of equations involving ψ

The variable $\psi_t^{(i)}(x)$ is defined to be the contribution to the expected local joint density $\bar{n}_t^{(2)}(x)$ from pairs of individuals with their most recent common ancestor at time i ($i < t$). The simplest initial distribution of individuals is a single individual released at the point $x = 0$ at time $t = 0$ so that $n_0(x) = \delta(x)$ and $\bar{n}_0^{(2)}(x) = 0$. The expected local joint density is then given as

$$\bar{n}_t^{(2)}(x) = \sum_{i=0}^{t-1} \psi_t^{(i)}(x), \tag{51}$$

for $t > 0$, and thus (17) can be rewritten as (29).

The first term in equation (27) describes the joint density arising from siblings having identical parents. Using this term we see that

$$\psi_{i+1}^{(i)}(x) = \int_{-\infty}^{\infty} R_0^2 k^2(z-x) \left(n_i(z) - \epsilon \sum_{j=0}^{i-1} \psi_i^{(j)}(z) \right) dz. \tag{52}$$

The second term in equation (27) describes the propagation of this joint density during successive time steps. Using this term we see that

$$\begin{aligned} \psi_{i+2}^{(i)}(x) &= \int_{-\infty}^{\infty} R_0^2 k^2(y-x) \int_{-\infty}^{\infty} R_0^2 k^2(z-y) \left(n_i(z) - \epsilon \sum_{j=0}^{i-1} \psi_i^{(j)}(z) \right) dz\, dy \\ &= \int_{-\infty}^{\infty} R_0^4 k_1^2(z-x) \left(n_i(z) - \epsilon \sum_{j=0}^{i-1} \psi_i^{(j)}(z) \right) dz. \end{aligned} \tag{53}$$

Continuing in this manner yields equation (28).

When the factor β_m (40) is used to approximate (36) in equation (35) we have a variant of (27) with β_m multiplying the second term in (27). The value of the index m is given as the number of time steps previous at which individuals shared their most common ancestor. Thus we have

$$\psi_{i+1}^{(i)}(x) = \int_{-\infty}^{\infty} R_0^2 \beta_0 k^2(z-x) \left(n_i(z) - \epsilon \sum_{j=0}^{i-1} \psi_i^{(j)}(z) \right) dz, \tag{54}$$

$$\psi_{i+2}^{(i)}(x) = \int_{-\infty}^{\infty} R_0^4 \beta_0 \beta_1 k_1^2(z-x) \left(n_i(z) - \epsilon \sum_{j=0}^{i-1} \psi_i^{(j)}(z) \right) dz. \tag{55}$$

and so on. Continuing in this manner yields

$$\psi_{i+m}^{(i)}(x) = \int_{-\infty}^{\infty} R_0^{2m} \left(\prod_{j=0}^{m-1} R_0^2 \beta_j \right) k_{m-1}^2(z-x) \left(n_i(z) - \epsilon \sum_{j=0}^{i-1} \psi_i^{(j)}(z) \right) dz, \tag{56}$$

and this can be rewritten as (41).

C. Calculations with the composite normal kernel

The composite normal kernel

$$k(x) = pN(0, \sigma_1^2) + (1-p)N(0, \sigma_2^2) \tag{57}$$

has its $(n-1)$th fold convolution as

$$k_{n-1}(x) = \sum_{j=0}^{n} \binom{n}{j} p^j (1-p)^{n-j} N(0,\, j\sigma_1^2 + (n-j)\sigma_2^2). \tag{58}$$

The moment generating function of this convolution squared is

$$\hat{k^2}_{n-1}(s) = \sum_{j=0}^{n}\sum_{k=0}^{n} \frac{\binom{n}{j}\binom{n}{k} p^{j+k}(1-p)^{2n-j-k} \exp(\sigma_{jk}^2 s^2/2)}{\sqrt{2\pi((j+k)\sigma_1^2 + (2n-j-k)\sigma_2^2)}}, \tag{59}$$

where

$$\sigma_{jk} = \frac{(j\sigma_1^2 + (n-j)\sigma_2^2)(k\sigma_1^2 + (n-k)\sigma_2^2)}{(j+k)\sigma_1^2 + (2n-j-k)\sigma_2^2}. \tag{60}$$

References

1. Ball, F.: Coupling methods in epidemic theory. In: Mollison, D. (ed) Epidemic Models: Their Structure and Relation to Data, pp 34–52. Cambridge University Press, 1995
2. Bartlett, M.S.: Deterministic and stochastic models for recurrent epidemics, Proc. 6th Berkely Symp. on Math. Statist. and Prob. **4**, 81–109 (1956)
3. Bartlett, M.S.: Stochastic Population Models in Ecology and Epidemiology. Methuen, London, 1960
4. Bartlett, M.S.: An Introduction to Stochastic Processes with Special Reference to Methods and Applications. Cambridge University Press, Cambridge 1966
5. Biggins, J.D.: The asymptotic shape of the branching random walk, Adv. Appl. Prob. **10**(1), 62–84 (1977)
6. Biggins, J.D.: How fast does a general branching random walk spread? In: Athreya, K.B. and Jagers, P. (eds) Classical and Modern Branching Processes, pp 19–39. Springer, 1998
7. Cox, J.T., Durrett, R.: Limit theorems for the spread of epidemics and forest fires, Stoch. Processes Appl. **30**, 171–190 (1988)
8. Daniels, H.E.: The advancing wave in a spatial birth process, J. Appl. Prob. **14**, 689–701 (1977)
9. Durrett, R.: Spatial epidemic models. In: Mollison, D. (ed) Epidemic Models: Their Structure and Relation to Data, pp 187–201. Cambridge University Press 1995
10. Ellner, S.P., Sasaki, A., Haraguchi, Y., Matsuda, H.: Speed to invasion in lattice population models: pair-edge approximation. manuscript, 1998
11. Hardin, D.P., Takac, P., Webb, G.F.: Dispersion population models discrete in time and space, J. Math. Biol. **28**, 1–20 (1990)
12. Hardin, D.P., Takac, P., Web, G.F.: Asymptotic properties of a continuous-space discrete–time population model in a random environment, Bull. Math. Biol. **26**, 361–374 (1988)

13. Hardin, D.P., Takac, P., Webb, G.F.: A comparison of dispersal strategies for survival of spatially heterogeneous populations, SIAM J. Appl. Math. **48**(6), 1369 (1988)
14. Hastings, A., Higgins, K.: Persistence of transients in spatially structured ecological models, Science, **263**, 1133–1136 February (1994)
15. Hengeveld, R.: Dynamics of Biological Invasions. Chapman and Hall, London, 1989
16. Kot, M.: Diffusion-driven period doubling bifurcations, BioSystems, **22**, 279–287 (1989)
17. Kot, M., Schaffer, W.M.: Discrete-time growth-dispersal models, Mathematical Biosciences, **80**, 109–136 (1986)
18. Kot, M.: Discrete-time travelling waves: Ecological examples, J. Math. Biol. **30**, 413–436 (1992)
19. Kot, M., Mark, A., Lewis, van den Driessche, P.: Dispersal data and the spread of invading organisms, Ecology, **77**(7), 2027–2042 (1996)
20. Lewis, M.A., Pacala, S.: Modeling and analysis of stochastic invasion processes. J. Math. Biol. **41** (same issue), 387–429 (2000) (DOI: 10.1007/s002850000050)
21. Lui, R.: A nonlinear integral operator arising from a model in population genetics, I. lcmonotone initial data, SIAM J. Math. Anal. **13**(6), 913–937 (1982)
22. Lui, R.: A nonlinear integral operator arising from a model in population genetics, II Initial data with compact support, SIAM J. Math. Anal. **13**(6), 938–953 (1982)
23. Lui, R.: Existence and stability of travelling wave solutions of a nonlinear integral operator, J. Math Biol. **16**, 199–220 (1983)
24. McKean, H.P.: Application of Brownian motion to the equation of Kolmogorov-Petrovskii-Piscounov, Commun. Pure Appl. Math, **28**, 323–331 (1975)
25. Metz, J.A.J., van den Bosch, F.: Velocities of epidemic spread. In: Mollison, D. (ed) Epidemic Models: Their Structure and Relation to Data, pp 150–186, Cambridge University Press, 1995
26. Mollison, D.: The rate of spatial propagation of simple epidemics. In: Proc. 6th Berkeley Sym. Math. Stat. Prob., volume 3, pp 579–614. Univ. Calif. Press, Berkeley, 1972
27. Mollison, D.: Spatial contact models for ecological and epidemic spread, J.R. Statist. Soc. B, **39**(3), 283–326 (1977)
28. Mollison, D.: Markovian contact processes, Advances in applied probability, **10**, 85–108 (1978)
29. Mollison, D.: Dependence of epidemic and population velocities on basic parameters, Mathematical Biosciences, **107**, 255–287 (1991)
30. Moody, M.E., Mack, R.N.: Controlling the spread of plant invasions: the importance of nascent foci, Journals of Applied Ecology, **25**, 1009–1021 (1988)
31. Murray, J.D.: Mathematical Biology, volume 19 of Biomathematics. Springer-Verlag, New York, 1989
32. Neubert, M.G., Kot, M., Lewis, M.: Dispersal and pattern formation in a discrete-time predator-prey model, Theor. Pop. Biol., **48**(1), 7–43 (1995)
33. Pacala, S.W., Levin, S.A.: Biologically generated spatial pattern and the coexistence of competing species. In: Tilman, D. and Kareiva, P. (eds) Spatial ecology: The role of space in population dynamics and interspecific interactions, pp 204–232. Princeton University Press, 1998
34. Shigesada, N., Kawasaki, K., Takeda, Y.: Modeling stratified diffusion in biological invasions, American Naturalist, **146**, 229–251 (1995)
35. Slatkin, M.: Gene flow and selection in a cline, Genetics, **75**(3), 733–756 (1973)
36. van den Bosch, F., Metz, J.A.J., Diekmann, O.: The velocity of spatial population expansion, J. Math. Biol., **28**, 529–565 (1990)

37. Weinberger, H.F.: Asymptotic behavior of a model in population genetics. In: Chadam, J.M. (ed) Lecture Notes in Mathematics No. 648: Nonlinear Partial Differential Equations and Applications, pp 47–96. Proceedings Indiana 1967–1977 (1978)
38. Weinberger, H.F.: Long-time behavior of a class of biological models, SIAM journal on mathematical analysis, **13**(3), 353–396 May (1982)